Fifty Years of Wind Engineering

Prestige Lectures from the Sixth European and African Conference on Wind Engineering

Editors: C J Baker, D M Hargreaves, J S Owen and M Sterling

Fifty Years of Wind Engineering: Prestige Lectures from the Sixth European and African Conference on Wind Engineering

Chairs: J S Owen and M Sterling

Editors: C J Baker, D M Hargreaves, J S Owen and M Sterling

ISBN-13: 9780704428348

Typeset using the LaTeX typesetting system by D M Hargreaves

Foreword

Prof. Chris Baker, The University of Birmingham

Much has changed since 1963. In international terms political power was in the hands of the generation who had lived through the second-world war, and the scars of that war were still very noticeable across Europe. The stand-off between east and west known as the cold war was at its height, and the Cuban missile crisis still fresh in people's minds. In social terms there was a broad social democratic consensus across Europe, with the state playing a major role in industry, education, transport and many other sectors.

The subject of wind engineering, in so far as it had reached any level of self definition, mirrored the society in which its practitioners lived. Research work was concentrated in the state owned research laboratories the National Physical Laboratory and the Building Research Station in the UK for example - and the concerns were those of the society around it. A glance at the contents of the 1963 meeting on Wind Effects on Buildings and Structures held at the National Physical Laboratory in Teddington will reveal these interests. In that contents list we see papers on the design of long span bridges, necessary for the development and reinvigoration of long distance transport links; the need to eliminate conductor cable galloping to make the electricity supply network more resilient; and the need to develop codes of practice so that the housing stock could be improved and able to withstand gales such as the fiercely destructive Sheffield gale of 1962.

Whilst wind engineering has a long history, arising from incidents such as the Tay Bridge and Tacoma Narrows collapse, with solid foundational work carried out by the likes of Prandtl and von Karman in Germany, Eiffel in France, Irminger and Rathbun in the USA, Jensen in Denmark and Scruton in the UK, in 1963 new ideas and concepts were being formulated, and young researchers were arriving on the scene who were to have a major influence on the future of the discipline. Most notable amongst these was Alan Davenport who made a major contribution to the 1963 NPL meeting, and who, through the conceiving and the development of the "wind loading chain" was to make such a major contribution to the general development of the discipline. The meeting also saw discussion of many things we now take for granted - not least the development of wind tunnel boundary layer simulations in large environmental wind tunnels, which at that time was still a developing technology, if no longer a novelty.

The 1963 meeting thus marks a pivotal moment in the development of wind

engineering, and it is appropriate to mark the 50^{th} anniversary of that meeting as part of the 2013 European and African Conference on Wind Engineering. The chapters of this volume contain the keynote lectures from this conference that review the development of six key themes in wind engineering over the 50 years since the 1963 conference, and describe the current state of the art. Our understanding of the atmospheric boundary layer is fundamental to Wind Engineering and Prof. Barlow helpfully reminds us that in 1963 there was significant debate on how best to represent it to determine wind loads for design. She also highlights how the rapid advance in instrumentation is providing new data that is transforming our understanding of this key area today. Such understanding will feed into the next generation of wind loading codes, which were in their infancy in 1963. Now, in Europe at least, national codes have been overtaken by the Eurocode and Dr Hansen outlines in this volume the plans for further harmonisation. The last fifty years have seen great changes and developments in both buildings and bridges. Prof. Borri charts our growing understanding of wind effects on bridges and Prof. Letchford reminds us that we face new challenges and many issues remain unresolved. In 1963, the tool of choice for wind engineering research was the wind tunnel. Prof. Diana illustrates how technological developments have continued to improve the quality and quantity of experimental data and facilities have now been developed to investigate other extreme wind events such as downbursts. However, the intervening years have also seen the rise of Computational Wind Engineering, almost unheard of in 1963 but now, as Prof. Blocken shows, a major contributor to the development of the discipline.

It will be clear from reading these chapters that wind engineering in 2013 owes a very great deal to those who gathered at Teddington in 1963. Yet, those six themes remain the focus of much research today and it is also clear that the most recent developments offer the potential to transform the practice of wind engineering. In Cambridge in 2013 we gather for the sixth in the series of regional conferences organised under the auspices of the IAWE. Delegates from 20 nations around the world have contributed over 120 papers that continue in the vibrant and successful tradition of the previous conferences in Guernsey, Genoa, Eindhoven, Prague and Florence. It is our hope that in 2063 wind engineers will look back on EACWE 2013 as another pivotal moment in the development of the discipline, but in doing so we remember the words of one of Cambridge's greatest scholars, "If I have seen further it is by standing on the shoulders of giants."

Distinguished Lecturers

Professor Janet Barlow

Janet Barlow is Professor of Environmental Physics at the Department of Meteorology at the University of Reading. She has interests in urban meteorology, turbulence, remote sensing of the boundary layer and novel experimental techniques in both wind tunnel and the field.

Professor Bert Blocken

Bert Blocken is full professor and holds the Chair of Building Physics at Eindhoven University of Technology in the Netherlands. His main areas of expertise are Urban Physics and Environmental Wind Engineering.

Professor Claudio Borri

Claudio Borri is full professor of Computational Mechanics of Structures, University of Florence (Italy) and Vice-President of the Interuniversity Research Centre on Building & Environmental Aerodynamics.

Professor Giorgio Diana

Giorgio Diana is Professor Emeritus of Applied Mechanics at Politecnico di Milano. He is Director of the Research Centre for Wind Engineering (CIRIVE), whose wind tunnel is the largest boundary Layer Wind Tunnel in Europe.

Dr Svend Ole Hansen

Svend Ole Hansen is director and founder of Svend Ole Hansen ApS and has been a lecturer in wind engineering at the Technical University of Denmark and Syddansk University. His text books on wind engineering are widely read and well regarded.

Professor Chris Letchford

Chris Letchford is Professor and Head of Department of Civil & Environmental Engineering at Rensselaer Polytechnic Institute. His research interests cover a wide range of wind effects on structures including thunderstorm downbursts and tornadoes.

Scientific Committee Members

Dr J Macdonald (Chairman, UK)
Dr A Quinn (Secretary, UK)
Prof. G Augusti (It)
Dr J Barlow (UK)
Prof. J Bogunovic-Jakobsen (Nor)
Prof. C Borri (It)
Prof. A Flaga (P)
Dr O Flamand (Fr)
Dr C Georgakis (Dk)
Dr C Geurts (NL)
Dr A Goliger (RSA)
Dr G Grillaud (Fr)
Prof. R Hoeffer (Ger)
Dr J Holmes (Aus)
Prof. N Jones (USA)
Prof. A Kareem (USA)
Prof. K Kwok (Aus)
Prof. C Letchford (USA)
Prof. J Naprstek (Cz)
Prof. H-J Niemann (Ger)
Dr A Palmeri (UK)
Prof. U Peil (Ger)
Dr S Pospisil (Cz)
Prof. P Richards (NZ)
Prof. G Solari (It)
Prof. T Stathopoulos (Can)
Prof. Y Tamura (Jap)
Dr I Taylor (UK)
Dr N Waterson (UK)
Dr Z-T Xie (UK)
Prof. A Zasso (It)

Contents

2

Wind Loading Design Codes

S.O. Hansen

2.1 Introduction

In 1963, at the time of the first international conference on wind effects on structures held in UK, the wind loading design codes were typically a few pages long, and they covered only a few simple structures. As an example the first Danish wind code was published in 1945, and it specified static wind load acting on selected structural geometries. In the revised Danish wind code published in 1966, specifications of gust factors for dynamic sensitive structures and vortex shedding were added. The codified gust factor approach followed the model originally established by Alan G. Davenport in the beginning of the sixties, see Davenport (1962) and Davenport (1967), and in the following years, this model was widely acknowledged and applied in many national wind loading design codes.

In 1963 most pressure and force coefficients were still obtained from wind tunnel testing carried out in smooth flow. Although Martin Jensen's model law "The flow in the wind tunnel should be turbulent in the same way as the flow in the natural wind" was put forward in the 1950s (Jensen, 1958), the construction of boundary layer wind tunnels applying it was in its initial phase. One of the first boundary layer wind tunnels able to generate scaled boundary layers in accordance with Martin Jensen's model law was constructed by Alan G. Davenport at University of Western Ontario in Canada in the early sixties, see Davenport and Isuymov (1968).

In the following years boundary layer wind tunnels were constructed worldwide. Wind tunnel tests were carried out with simple as well as with more complex structures, and the data obtained in these wind tunnel tests were used to extend the scope of the wind loading design codes and to make the specifications in much better compliance with full–scale conditions. However, there has been a lack of a common worldwide basis with consistent definitions for wind loading calculations, e.g. the wind climate has not been described using a common definition of terrain roughness and averaging time of the wind velocity, and the pressure and force coefficients have not been based on the same wind loading model. This lack of consistency has led to many wind loading design codes that provide somewhat different results. However, the deviations are in most situations relatively minor, and now the time seems to be mature for a harmonization of the many different wind loading design codes.

In Europe this process of harmonization was initiated around 1980-90 with the decision to prepare Eurocodes – see Section 2.2.

Many papers have dealt with comparisons between wind loads calculated using different wind loading design codes, such as Eurocodes, ISO codes and the ASCE codes, see e.g. Holmes et al. (2009) and Bashor and Kareem (2009). In the present paper, the main focus is put on the Eurocodes, and the main trends expected in future revisions.

2.2 Eurocodes

The present Eurocodes comprise more than sixty parts, one of them being the Eurocode on wind actions.

The first Eurocode on wind actions, ENV 1991-2-4:1995, was completed in 1995, and it was followed by a revised Eurocode version, EN 1991-1-4:2005 in 2005. The process of drafting the EN Eurocode on wind action was discussed by Zimmerli (2001) and selected background material of the drafting were outlined by Geurts et al. (2001) and by Hansen et al. (2001).

In the Eurocode EN 1991-1-4:2005, the specification of the characteristic wind load is structured in accordance with the wind load chain originally introduced by Alan G. Davenport, see Dyrbye and Hansen (1996) and Figure 2.1. This was decided in order to make the presentation as user friendly as possible.

The elements of the wind load chain are as follows:

1. The wind climate is specified by the basic wind velocity defined as the 10-minute mean wind velocity at 10 m height above reference terrain

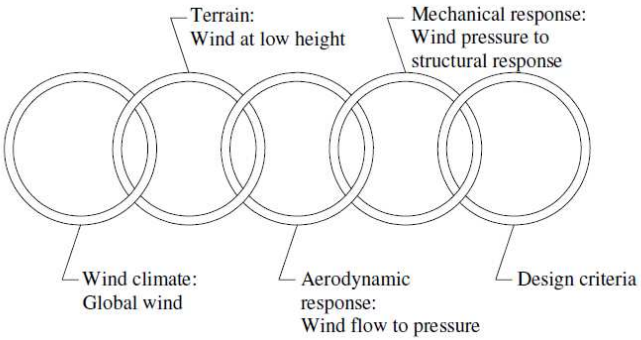

Figure 2.1: Wind load chain introduced by Alan G. Davenport.

with a roughness length of 0.05 m and having a return period of 50 years corresponding to an annual probability of exceedance of 0.02.

2. The terrain effects are specified by 5 standard flat terrains spanning from category 0 with a roughness length of 0.003 m to category IV with a roughness length of 1 m. Simplified rules for transition between terrains having different roughnesses and the effect of orography are included in the Eurocode. The extreme winds and terrain effects specified are used to calculate the peak velocity pressure, q_p , which is the basic parameter describing the incoming undisturbed airflow approaching the structure.

3. The aerodynamic response is determined by multiplying the peak velocity pressure by pressure coefficients and force coefficients specified for the different structural geometries.

4. The mechanical response defines the response of the structure, e.g. in form of deflections, accelerations and stresses.

5. The design criteria define the dimensioning criteria used to evaluate the mechanical response calculated.

The following sections focus on each of the different elements of the wind load chain.

The present Eurocodes do not cover phenomena such as transient wind conditions and thermal effects on the characteristic wind, e.g. strong arctic thermal surface inversion, hurricanes or tornadoes. Furthermore, torsional

vibrations, e.g. of tall buildings with a central core, vibrations where more than the fundamental mode needs to be considered, cable supported bridges and bridge deck vibrations from transverse wind turbulence are not covered in the Eurocodes. Some of these phenomena are planned to be included in the next Eurocode revision.

In each European member state the Eurocodes are applied together with its respective National Annex indicating that the present lack of harmonization is found by comparing the different National Annexes across Europe. National Annexes may provide meteorological information and select the Eurocode procedure that is actually to be applied in the design calculations. Part of the harmonization is to reduce the number of National Determined Parameters in future Eurocode revisions.

The European Committee for Standardization, CEN, plans to carry out a coordinated revision of the Eurocodes during the coming 3-5 years. Working Groups with representatives from different European countries are being established and the scope of the revisions is being discussed thoroughly. One of the key issues is to make the Eurocodes more user friendly by introducing simplifications wherever possible. In the planned Eurocode revision of EN 1991-1-4:2005 a part of the scope is to identify, and as far as possible to remove inconsistencies in determining wind actions and wind action effects on structures covered in different Eurocode Parts and in ISO standards. Aspects of the revision planned for EN 1991-1-4:2005 are discussed in the following sections.

In the Eurocodes partial safety factors are used to convert characteristic values to design values. For structures exposed to wind actions these partial safety factors should take the uncertainties of all elements of the wind load chain properly into account. Detailed calibration studies, see e.g. Vrouwenvelder and Scholten (2010), have shown that the partial safety factor on wind actions should be of the order of 1.7 and that the Eurocode partial safety factor for wind action specified to be 1.5 may actually underestimate the inherent uncertainties. However, this underestimation of approximately 10-15% is more than balanced out by safe estimates of characteristic values in some of the elements of the wind load chain, e.g. in the definition of design criteria, see Section 2.7 for further explanation.

2.3 Wind Climate

The wind map in Figure 2.2 shows basic wind velocities included in EN 1991-1-4:2005. The lack of harmonization across the borders of Europe in 1995 is

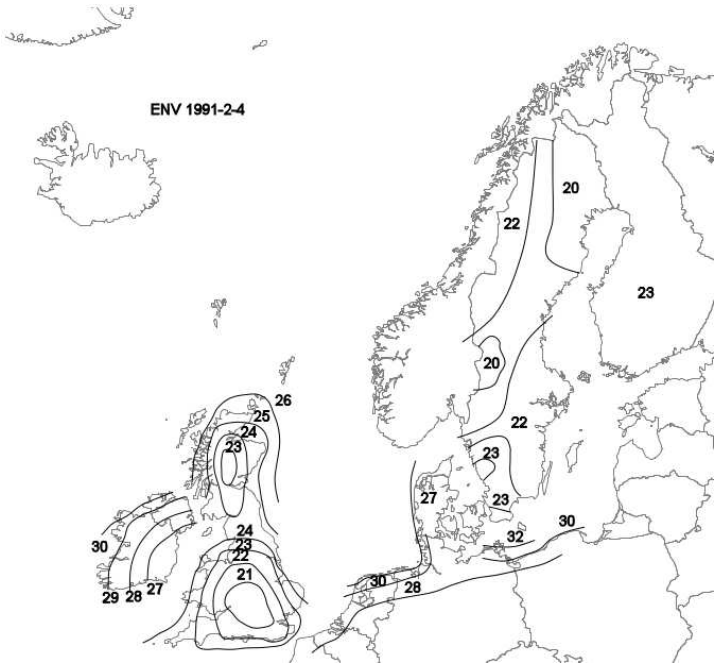

Figure 2.2: North European wind map of basic wind velocities ($\mathrm{m\,s^{-1}}$) in EN 1991-1-4:2005.

obvious. Some of the geographical areas lacking harmonization are:

1. The basic wind iso–velocity curves from different parts of UK are conflicting.

2. Denmark and Sweden on each side of the narrow Øresund strait specify a basic wind velocity of $27\,\mathrm{m\,s^{-1}}$ and $23\,\mathrm{m\,s^{-1}}$, respectively.

3. Denmark and Germany on each side of Fehmarn Belt specify a basic wind velocity of $27\,\mathrm{m\,s^{-1}}$ and $32\,\mathrm{m\,s^{-1}}$, respectively.

The obvious lack of harmonization shown in Figure 2.2 and the European aim of establishing harmonized structural codes have initiated many local studies of basic wind velocities using historical data. These studies have reduced or removed some of the sudden jumps across borders, see Figure 2.3.

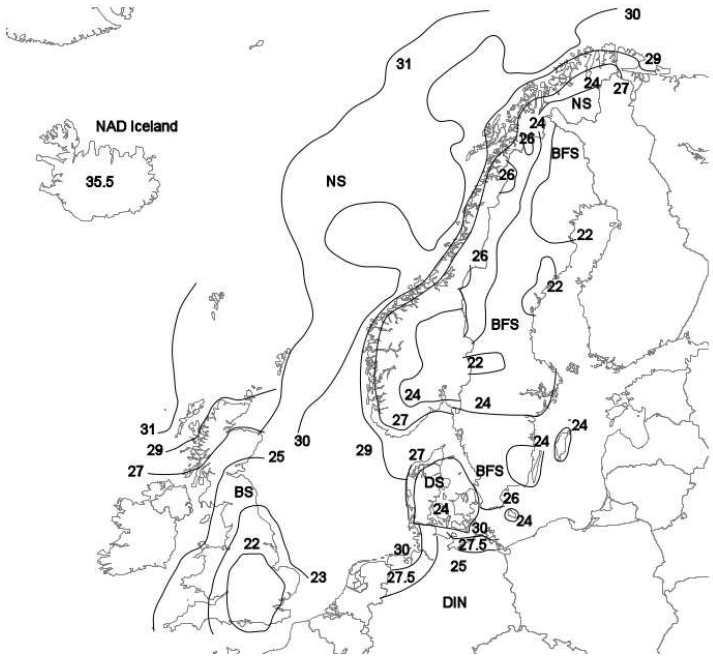

Figure 2.3: North European wind map of basic wind velocities ($\mathrm{m\,s^{-1}}$) according to National Annexes of EN 1991-1-4:2005.

There is now seen to be a reasonable good agreement between basic wind velocities specified in Norway, Denmark and Sweden. The specifications in UK are now internally consistent, and they are in reasonable agreement with extrapolations based on Scandinavian values. Not all parts of Europe show the same consistency across borders, and this may be shown in an updated wind map based on basic wind velocities specified in existing National Annexes and by emphasizing the wind map values, where differences across borders still exist. A map like that may urge local standards organizations to continue the harmonization process, e.g. for Germany and Denmark where the change in basic wind velocity crossing Fehmarn Belt is from $24\,\mathrm{m\,s^{-1}}$ in Denmark to $30\,\mathrm{m\,s^{-1}}$ in Germany.

Some member states have had to change their basic wind velocity definition to the Eurocode basis, i.e. a 10-minute mean wind velocity at 10 m height above a terrain with a roughness length of 0.05 m. Previously the UK, for

instance, used a 1 hour mean wind velocity at 10 m height above a terrain with roughness length of 0.03 m. However, the UK did not have to prepare a new wind map since the effect of changing the averaging time from 1 hour to 10 minutes balances out the effect of changing roughness length from 0.03 m to 0.05 m. The basic wind velocity defined in ISO 4354:2009 refers to a 10-minute mean wind velocity at 10 m height above a terrain with roughness length of 0.03 m, and unfortunately this definition deviates from the Eurocode basis.

The wind map data illustrated in both Figure 2.2 and 2.3 have mainly been based on historical data, and the effects of climate change have not been included on a consistent basis. Recently, extensive research programs have been carried out in order to establish a basis for determining the effect of climate change on the wind conditions. As an example the Danish Meteorological Institute have found that the basic wind velocity may increase by up to approximately 5% over the next 100 years if the most severe climate change scenarios turn out to be realistic. The modest influence of climate change on the basic wind velocity is confirmed by the trend indicated using the historical data illustrated in Figure 2.4.

The relatively minor influence of climate change seems to have been included already by the basic wind velocities conservatively estimated. However, climate change may increase the magnitude of frequent winds, and this may increase the importance of fatigue damage of wind sensitive structures. Climate change will be focused on in future Eurocode revisions.

2.4 Terrain Effects

The terrain effects include wind models for calculation of wind velocities and peak velocity pressures based on terrain roughness and orography, and also on terrain roughness transitions. The standard terrain categories specified in the Eurocode are illustrated in Figure 2.5, taken from EN 1991-1-4:2005. The illustrations of terrain categories I to IV were originally prepared by the Danish Standards Foundation.

The European Member States specify many different models for taking the transition between roughness categories into account. This topic is one of the main aspects for harmonization in the Eurocode revision planned.

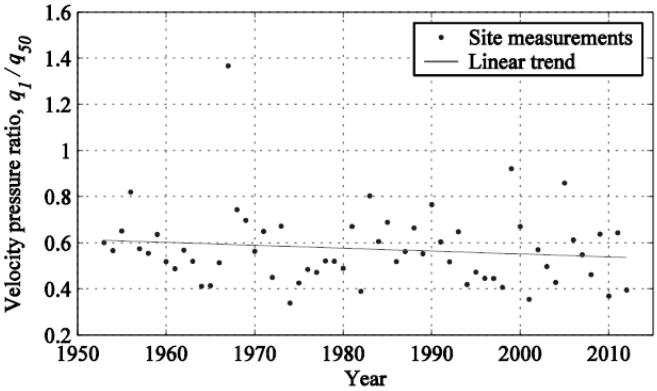

Figure 2.4: Annual extreme mean velocity pressures measured at 10 m height at Kastrup airfield in Denmark from 1953-2012 by the Danish Meteorological Institute. The annual extremes, q_l, have been normalized by the 50-year mean velocity pressure, q_{50}, based on the site measurements.

Category 0
Sea and coastal areas exposed to the open sea.
Roughness length 0.003 m.

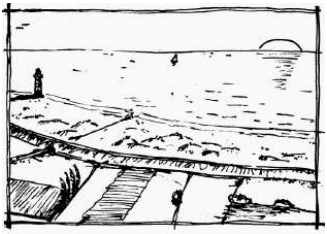

Category I
Lakes or areas with negligible vegetation and without obstacles.
Roughness length 0.01 m.

Category II
Areas with low vegetation such as grass and isolated obstacles (trees, buildings) with separations of at least 20 obstacle heights.
Roughness length 0.05 m.

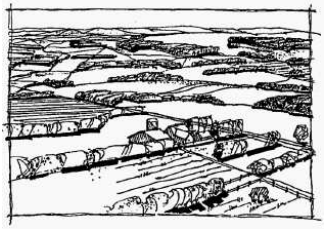

Category III
Areas with regular cover of vegetation or buildings or with isolated obstacles with separations of a maximum of 20 obstacle heights (such as villages, suburban terrain, permanent forest).
Roughness length 0.3 m.

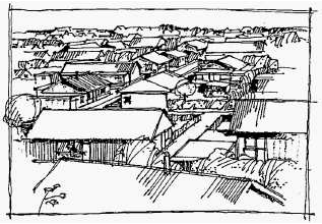

Category IV
Areas in which at least 15% of the surface is covered with buildings and their average height exceeds 15 m.
Roughness length 1.0 m.

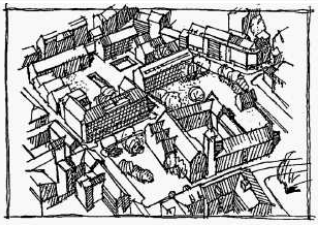

Figure 2.5: Terrain categories in EN 1991-1-4:2005.

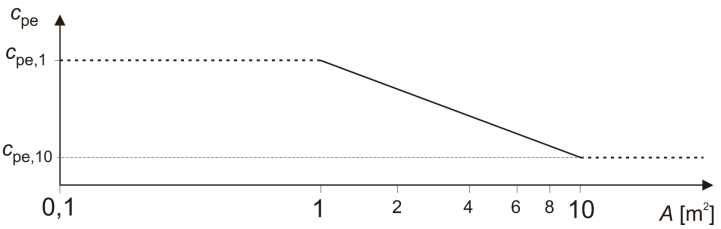

Figure 2.6: Recommended Eurocode procedure for determining the external pressure coefficient c_{pe} for buildings with a loaded area between $1\,\mathrm{m}^2$ and $10\,\mathrm{m}^2$.

2.5 Aerodynamic Response

The sections below focus on wind-induced pressures on a one skin façade and two skin façade, respectively, and the global wind load on a structure is also analysed.

In the planned revision of the Eurocode a systematic review of internal and external pressure coefficients, including influence areas and the zoning, will be carried out based on the current state of the art. Furthermore, force coefficients for global wind loads, e.g. for the design of foundations, will be included.

2.5.1 Wind–induced Pressures on a One Layer Façade

Cook (1985) has carried out a large number of wind tunnel measurements and simulations in order to answer the following question: *What is the value of the loading coefficient that results in a design load of the desired design risk, given a wind speed of the same risk?* Thus, for the external pressures the question is: *Which pressure coefficient c_{pe} provides a characteristic wind pressure calculated by $w_e = c_{pe}q_p$, in which q_p is the characteristic peak velocity pressure?* Cook (1985) found that the pressure coefficient should be obtained as the 78% fractile in the Gumbel distribution of pressure extremes.

As illustrated in Figure 2.6, the Eurocode specifies external pressure coefficients as a function of loaded area, and the tabulated values give $c_{pe,10}$ representing a loaded area of $10\,\mathrm{m}^2$ to be used for the wind load on the main structural elements, and $c_{pe,1}$ representing a loaded area of $1\,\mathrm{m}^2$ to be used in the design of fixings, smaller panels, etc.

The majority of the Eurocode pressure coefficients are based on Cook (1985) and Stathopoulos (1979) for $10\,\mathrm{m}^2$ and $1\,\mathrm{m}^2$ loaded areas, respectively.

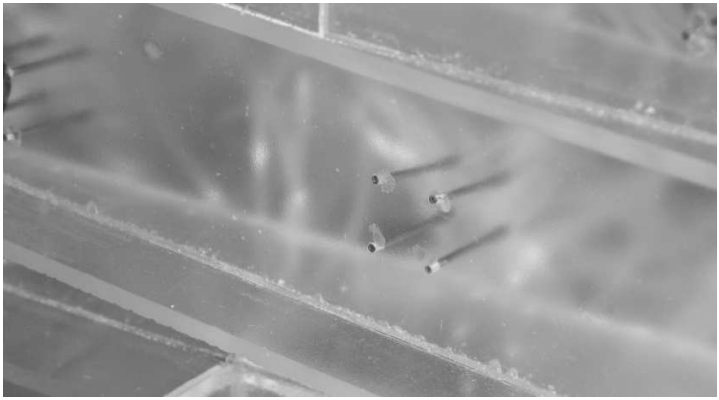

Figure 2.7: Photo of a pressure tap cluster on model. Each pressure tap has a full-scale equivalent area of less than $1\,m^2$.

Cook used time averaging for determining $10\,m^2$ wind loads indicating that these values have not been based directly on a spatial averaging.

After the publication of the EN 1991-1-4 in 2005, a large number of measurements have been carried out in our wind tunnel aimed at determining both $1\,m^2$ and $10\,m^2$ loads, as well as loads on intermediate areas, on a consistent basis. This has been accomplished by installing pressure tap clusters on the wind tunnel models, see Figure 2.7. The pressures in each pressure tap cluster have been measured simultaneously indicating that spatial averaging could be used to estimate the wind action in different areas of up to approximately $10\,m^2$. Thus, the procedure applied facilitates a determination of both $1\,m^2$ and $10\,m^2$ pressure coefficients, which could be compared directly to the same type of pressure coefficients specified in the Eurocode.

Typical trends for the loads measured on façades are:

- For $1\,m^2$ loaded areas the measurements show larger suctions than the Eurocode value of -1.4 for façades. This may partly originate from the fact that each pressure tap has an area of less than $1\,m^2$.

- For $10\,m^2$ loaded areas the measurements show lower suctions than the Eurocode value of -1.2 for façades. Thus, the spatial averaging applied in the wind tunnel gives larger reductions than the Eurocode.

The measurements illustrated in Figures 2.8 to 2.10 show two case studies,

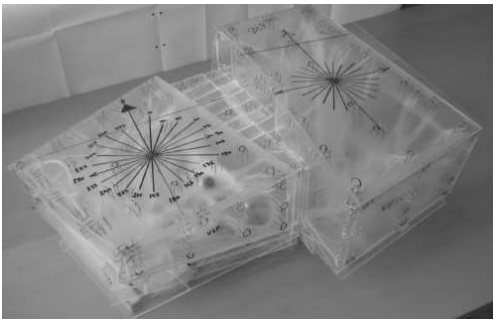

(a)

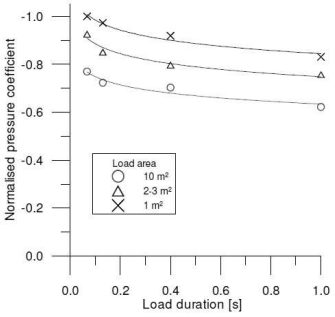

(b)

Figure 2.8: The Concert and Conference Centre "Harpa" in Reykjavik, Iceland: (a) photo of 1:200 wind tunnel scale model; (b) normalised pressure coefficients measured on the Eastern façade in separated zones with large suctions as function of load duration and load area. Reproduced by permission of Ramboll Denmark, Consulting Engineers of the building.

where the influence of both time averaging and spatial averaging of simultaneously measured external pressures are illustrated.

The effect of spatial averaging and time duration for pressures measured at Søndermarken is shown in Figure 2.10. In this figure, the time duration has been made non-dimensional by multiplying it with the mean wind velocity divided by the dimension e from the Eurocode – the minimum of 2 heights and the cross wind dimension determining the sizes of the different zones on the structure. This choice of length scale has been found to be in good agreement with measurements carried out in the separated zones with large suctions on different models.

Figures 2.8(b) and 2.10 show examples of characteristic pressure coefficients as function of load durations for loaded areas of $1\,m^2$, 2 to $3\,m^2$ and $10\,m^2$, respectively. The effect of load duration is significant for all loaded areas considered, indicating that the largest suction peaks have very short durations of the order of 0.1 s. Especially for short durations the averaging effect is pronounced. It may be observed that the pressure coefficient is approximately 30 to 40% smaller for the $10\,m^2$ loads with duration of approximately 1 s compared to its value for $1\,m^2$ loads with duration of approximately 0.1 s. A consistent approach with data sets including both the effect of duration and loaded area are needed. The data presented show the importance of

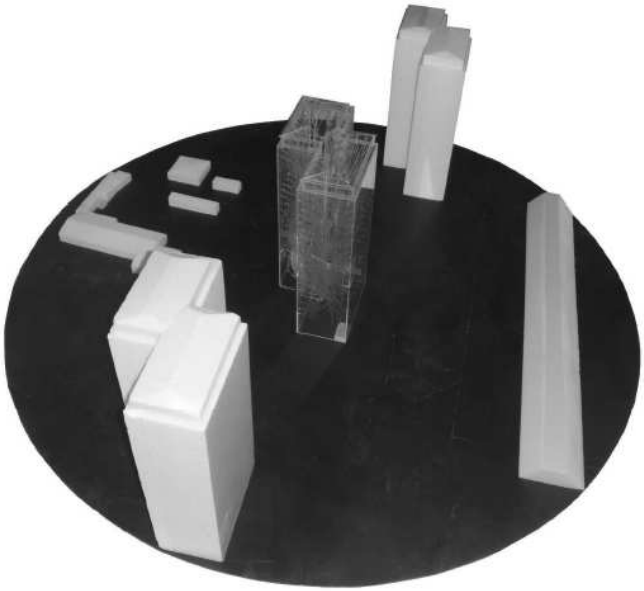

Figure 2.9: Photo of a 1:200 wind tunnel scale model of a block building in Søndermarken in Copenhagen, Denmark. The pressure tap model is situated in the middle of the circle. Reproduced by permission of Moe, Consulting Engineers, and the building owner, KAB.

both load duration and spatial averaging.

More accurate design calculations may be carried out if the wind load data could be combined with structural resistances as function of load durations. However, the resistance data available for most structures are not sufficiently accurate to support a detailed design of this nature. Thus, the structural resistances are often underestimated for the short duration loads indicating that the present approach is conservative. However, it is not possible to quantify the actual degree of conservatism at present. This is discussed further in Section 2.7.

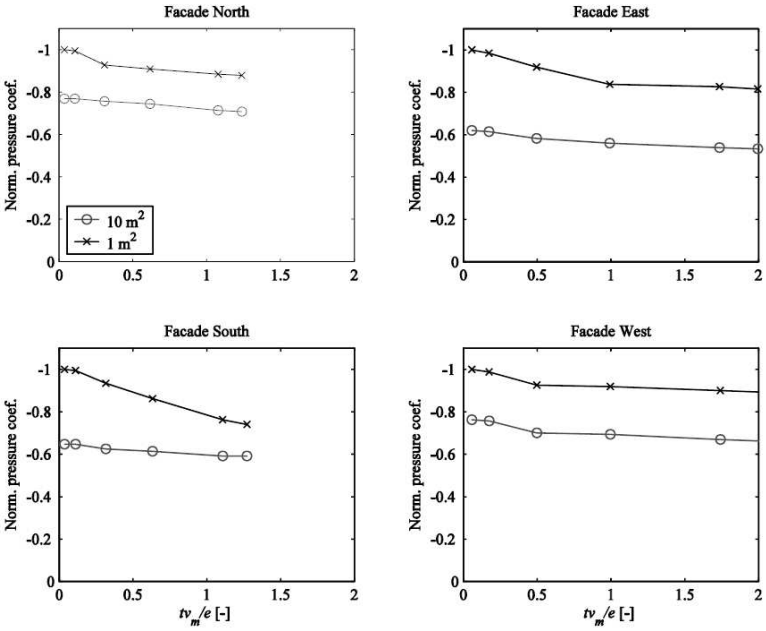

Figure 2.10: Normalised pressure coefficients from measurements of façade wind loads on a structure. The nondimensional x-axis is averaging time, t, multiplied by the mean wind velocity, v_m, and divided by the Eurocode-defined dimension of e. Reproduced by permission of Moe, Consulting Engineers, and the building owner, KAB.

2.5.2 Wind–induced Pressures on a Two Skin Façade

The data provided in the Eurocode for two skin façades is based on ECCS (1987). However, the background needs to be extended with further test results in order to cover the typical full-scale situations sufficiently accurately.

The two skin façade considered here has an impermeable inside skin and a permeable outside skin. The wind-induced pressures on the two skin façade depend on many geometrical parameters, such as the distance between the layers and the permeability of the outside skin. The Eurocode recommends that there are no openings at the extremities of the layer between the skins, and in this situation the specifications are given for distances between the skins of less than 100 mm and when the outside skin has approximately uniformly

Figure 2.11: 1:25 scale model of two skin façade of a block building in Søndermarken in Copenhagen. The photo shows the model in the large wind tunnel of SOH Wind Engineering in Vermont, USA. The vertical oriented cavity is shown in the middle of the photo, where the model is constructed of plexiglass. Reproduced by permission of Moe, Consulting Engineers, and the building owners, KAB.

distributed openings. According to the Eurocode the net pressure coefficient for overpressure and under pressure are 2/3 and 1/3 of the external pressure coefficient, respectively.

An example with an inner impermeable skin and an outer permeable skin at a distance of 50 mm has been carried out in a large wind tunnel on a scale of 1:25, see Figure 2.11. The permeability of the outer skin is approximately 10%. The air flow in the cavity is mainly able to move vertically due to vertical barriers from top to bottom.

Figure 2.12 shows the pressures measured in the wind tunnel tests carried out simulating a relatively low turbulent flow. The net pressure acting on the outer skin is determined as the difference between the two curves on each of the two plots in Figure 2.12. The results presented in the figure show net pressure coefficients on the outer skin being less than 0.1, i.e. much lower values than specified in the Eurocode. Thus, the pressure equalization is much more effective than assumed in the Eurocode for the particular geometry investigated.

The net pressures have also been determined by CFD using boundary

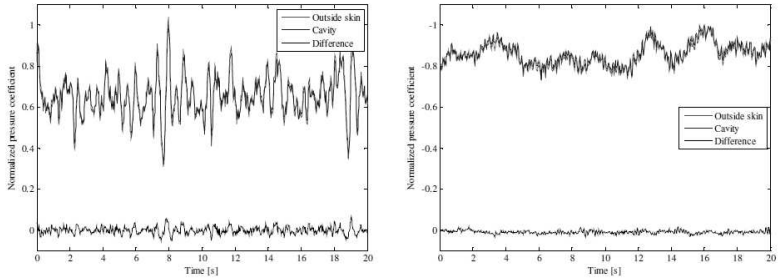

Figure 2.12: Normalised external pressures on outside skin and normalised cavity pressures as function of time for a two skin façade. The net pressures acting on the outside skin are determined as the pressure difference illustrated by the black curves. Left-hand side: Pressures in windward side. Right-hand side: Pressures in separated zone with large suctions on along-wind side. Reproduced by permission of Moe, Consulting Engineers, and the building owner KAB.

pressure conditions measured in a wind tunnel in turbulent flow on a model with an impermeable skin. These CFD calculations confirm that the pressure equalization is very efficient for the present geometrical configuration, and that the net pressures become insignificant.

Measured pressure coefficients for the many different geometrical configurations possible are needed in order to establish a sufficiently broad code basis. The results above are one example where the pressure equalisation across the external outer skin is very effective in reducing the wind action on this skin.

2.5.3 Wind–induced Global Loads

The characteristic wind load, F_w, acting on the structure is determined by the following expression specified in the Eurocode EN 1991-1-4:2005,

$$F_w = q_p c_s c_d c_f A_{\text{ref}},$$

where q_p is the characteristic peak velocity pressure at reference height, $c_s c_d$ is the structural factor, c_f is the force coefficient, and A_{ref} is the reference area. The structural factor comprises of a size effect expressed by c_s and a dynamic amplification effect given by c_d in the Eurocode.

The background of the two models presented in the Eurocode for detailed calculations of the structural factor in dynamic response is documented by

Solari (1993a,b) and Hansen and Krenk (1999), respectively. The models are based on the approach originally established by Davenport – see Davenport (1962) and Davenport (1967).

Figure 2.13 shows a wind tunnel model where different size effects have been determined based on wind tunnel measurement. The test results illustrated below have been measured with a wind direction being perpendicular to the largest facade. The turbulent boundary layer air flow simulated has a roughness length of approximately 0.02 m.

The local pressures and suctions measured are illustrated in Figure 2.14. Figure 2.15 shows time histories of pressures averaged spatially over half of the windward and leeward façades, respectively. The Eurocode size factor, c_s, applied in Figure 2.15 has been calculated using Eurocode method 2 for dynamic response with a structure height of 20.2 m and a cross-wind width of 26.8 m (53.6/2) corresponding to the area of the spatially averaged pressures. The turbulent length scale calculated was 102 m based on the Eurocode for the air flow simulated.

Figure 2.14 shows that the Eurocode is in good agreement with the local pressures and suctions measured on the windward and leeward sides of the building. However, Figure 2.15 shows smaller global force coefficients for both the windward side and the leeward side compared to the Eurocode values. In the right-hand figure the Eurocode has been interpreted by multiplying the size factor of a side with the Eurocode factor of 0.85 taking the lack of correlation between windward side and leeward side into account. This interpretation is seen to be conservative for the total force adding pressures on the windward side to suctions on the leeward side.

The small variations of the averaged suctions on the leeward side are due to a small length scale mainly originating from the dimensions of the structure and not from the incoming air flow. The Eurocode dimension of e is often a relatively good estimate of a representative length scale on sides located in the zones governed by separated flows, see Section 2.5.1.

As described above the present Eurocode gives guidance for taking lack of correlation between pressures acting on the windward side and leeward side, respectively, into account when calculating wind actions on buildings. However, for reasons of simplification this effect has not been included in the Eurocode methods for calculating the structural factor for structural elements, where the forces are specified by force coefficients. This lack of consistency between forces based on pressure coefficients and force coefficients, respectively, may be removed in the Eurocode revision planned.

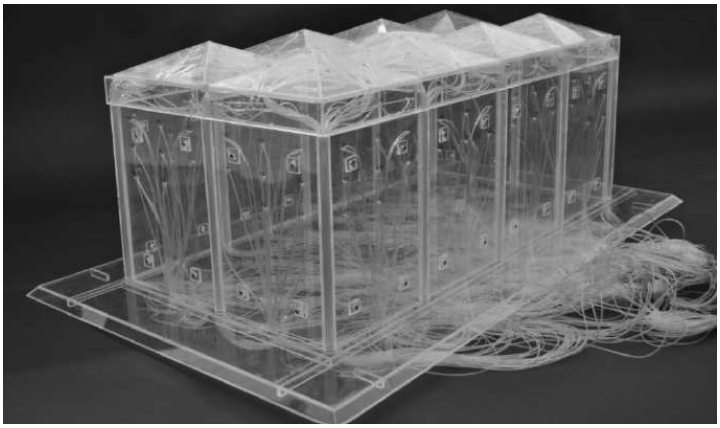

Figure 2.13: Wind tunnel model on a scale of 1:75. The façade height × width × depth is 20.2 × 53.6 × 27.2 m. Reproduced by permission of SiteCover.

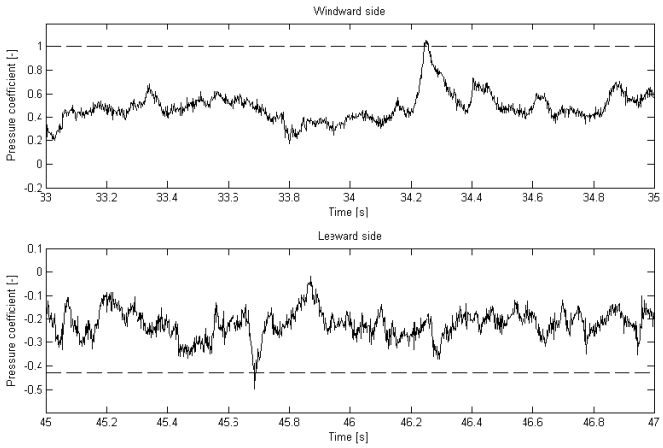

Figure 2.14: Coefficient for local pressure and suction measured at windward and leeward sides, respectively. The dotted lines indicate Eurocode pressure coefficients of 1.0 and -0.43. Reproduced by permission of SiteCover.

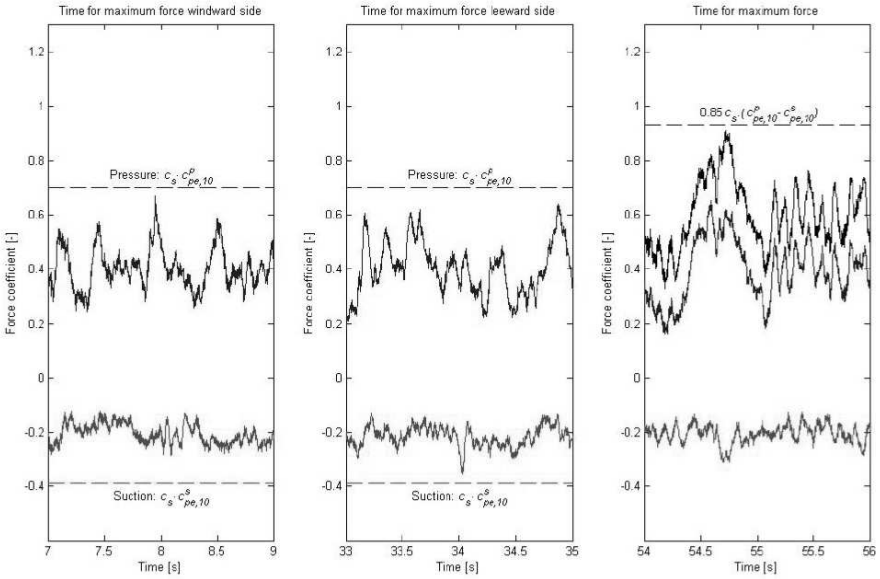

Figure 2.15: Left-hand figure and middle figure show coefficients for averaged pressure on windward side and leeward side, respectively. Right-hand figure also includes averages of the total coefficient adding pressures on windward side to suctions on leeward side. The dotted lines indicate Eurocode pressure coefficients: $c_s = 0.91$, $c^P_{pe,10} = 0.77$ and $c^P_{pe,10} = -0.43$. Reproduced by permission of SiteCover.

2.6 Mechanical Response

The mechanical response described below focus on some of the topics judged to be most important to modify in the panned Eurocode revision:

1. Influence lines or mode shapes with changing signs.
2. Vortex-induced vibrations.
3. Galloping-induced vibrations.
4. Special issues with cross section ratio 1:2, where vortex-induced and galloping-induced vibrations interact.

These topics are covered in the following sections.

2.6.1 Influence Lines or Mode Shapes with Changing Signs

The present Eurocode does not cover structures where influence lines or mode shapes have changing signs. In order to calculate accurate wind actions on structures such as torsionally sensitive high-rise buildings, multi-span bridges and guyed masts, specifications for influence lines or mode shapes changing signs will be included in the revised Eurocode. Thus, the scope of the Eurocode will be extended by the new specifications. The challenge of establishing these new specifications is the conversion of existing background information given in text books, see for example, Dyrbye and Hansen (1996), to user friendly codified rules.

2.6.2 Vortex-induced Vibrations

For a code, the most important aspect with respect to aeroelastic phenomena may be to specify a simple rule describing whether the structure to be designed may be susceptible to large vibrations. This is the main focus behind describing the influence of the general non-dimensional mass-damping parameter Sc_G defined by

$$Sc_G = \frac{2\delta_s m_e}{\rho b d}, \tag{2.1}$$

where ρ is the air density, δ_s quantifies the structural damping by the logarithmic decrement, which is approximately $2\pi\xi_s$, where ξ_s is the structural damping ratio, b is the crosswind width, d is the alongwind depth and m_e is the mass of the structure per unit length. When d is equal to b, this parameter is identical to the Scruton number, $Sc = 2\delta_s m_e/\rho b^2$.

Traditionally the Scruton number has been used to determine effects of motion-induced vortex shedding wind loads acting on structures, but as it depends on the cross-wind dimension only, and not on the in-wind dimension, the Scruton number does not contain any information on the wind load exposed length. Instead Hansen (2013) and Hansen (2011) propose to base the evaluations on the general non-dimensional mass-damping parameter, which includes the wind load exposed length and describes effects of motion-induced wind load consistently for different structures. This general non-dimensional mass-damping parameter may be derived by assuming that the motion-induced wind load is proportional to the wind load exposed length being equal to the in-wind dimension. Wind tunnel tests carried out with section models having the cross sections illustrated in Figure 2.16 confirm that it describes effects of motion-induced wind load more consistently than the Scruton number normally applied. The special issues of cross section 1:2 deliberately excluded from Figure 2.16 are described in Section 2.6.4.

Figure 2.17 shows the vortex-induced vibrations measured in the wind tunnel at the resonance wind velocity after build-up. The vibrations are expressed by the standard deviation, σ_y, of the displacement normalised by the cross-wind dimension, b, and the two illustrations are based on the same wind tunnel test results, however, plotted as function of the Scruton number and the general mass-damping parameter, respectively.

For low Scruton numbers galloping vibrations may occur at wind velocities below the resonance wind velocity for vortex shedding. However, these Scruton numbers are well below the Scruton numbers at which vortex-induced vibrations are illustrated in Figure 2.17.

The largest amplitudes in Figure 2.17 are seen to be highly dependent on the cross-sectional shape. It is not surprising that the bridge-like cross sections experience the smallest vibrations since increasing vibration amplitudes changes the air flow pattern for even small relative angles of attack for these types of cross section. The largest vibrations are observed for the cross sections of 1:1, 2:1 and 4:1. Large vibrations for square cross sections are confirmed in studies by others, see e.g. Hjorth-Hansen and Kyrkjeeide (1978), Kawai (1992), Scruton (1981) and Scruton (1963).

In typical designs the most interesting aspect of Figure 2.17 is to determine the mass damping parameters at which the vibrations start to occur. It is seen from the left-hand figure that vibrations starts to occur when the Scruton numbers are in the range of approximately 5 to 100, i.e. a very large range of critical Scruton numbers depending on the actual cross section in question. The general non-dimensional mass-damping parameter applied in the right-hand figure narrows down the critical mass-damping parameter range to be

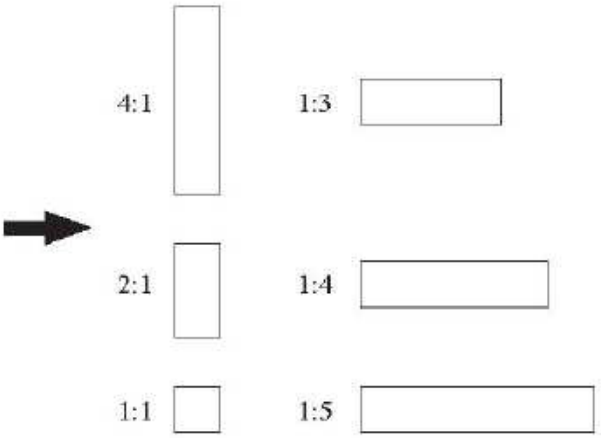

Figure 2.16: Cross sections tested (Hansen, 2011, 2013). Turbulence intensity in the tests was approximately 2%.

approximately 25 to 50 when the 1 : 5 bridge-like cross section is excluded. It seems that the assumption of a damping force being proportional to the along-wind depth may be too conservative for rectangular bridge-like cross sections, when the along-wind dimension is more than 4 to 5 times the cross-wind dimension. This is not surprising remembering that the vortices are generated at the upstream edges giving vortex shedding forces mainly acting at the upstream part of the cross section located in the vortex regions at top and bottom.

The cross sections of 4:1, 2:1 and 1:1 experience very large vibrations and standard deviations of approximately 10% of their cross-wind dimension occur for Scruton numbers in the range of approximately 5 to 30. The equivalent range of the general non-dimensional mass-damping parameter is approximately 25 to 30, i.e. a much smaller range.

The narrow ranges of the general non-dimensional mass-damping parameter facilitates that vortex-induced vibrations of the rectangular cross sections may be predicted by a theoretical model having only small variations in the parameters used in the calculations. Using the general non-dimensional mass-damping parameter rather than the Scruton number in analytical calculations hence makes the specific geometry less important when representative aero-

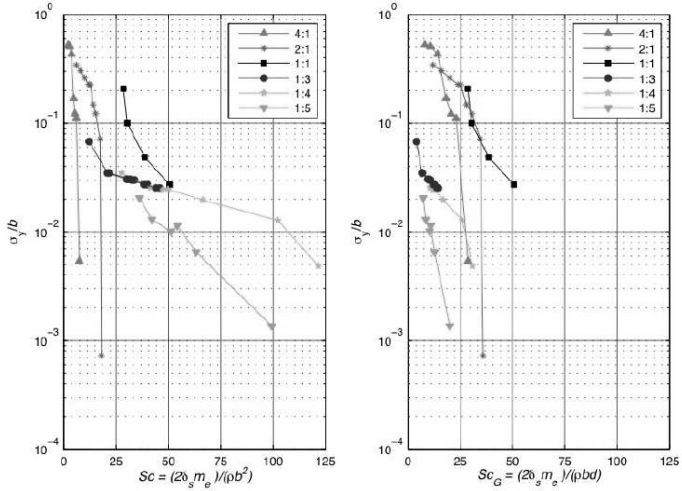

Figure 2.17: Vortex-induced vibrations measured. The Scruton number is used as x-axis in the left-hand figure, the general mass-damping parameter in the right-hand figure. From Hansen (2011) and Hansen (2013).

dynamic parameters are determined, see Hansen (2013).

Future revisions of the Eurocode on wind actions may include the general nondimensional mass-damping parameter predicting vortex-induced vibrations of different structures. This will reduce the uncertainties involved in the response predictions.

BD 49/01 gives rules for calculating vortex-induced response of different bridge cross sections, and the non-dimensional mass-damping parameter applied in BD 49/01 is found by replacing db with $b^{1.5}d^{0.5}$ in Equation 2.1. However, for a certain cross section their model specifies response amplitudes being inversely proportional to the structural damping, which is very different from the abrupt change from large to small vibrations indicated by the measurements presented in Figure 2.17. Furthermore, the results presented in Figure 2.17 show that BD 49/01 may underestimate the response, e.g. for 1:1 cross sections, where BD 49/01 specifies amplitudes 10 times smaller than the measurements for $Sc_G = 25$. For more bridge-like cross sections of say 1:4 the agreement between BD 49/01 and the results of Figure 2.17 is better.

The special aeroelastic effects for 1:2 cross sections outlined in Section 2.6.4 are not considered by BD 49/01.

2.6.3 Galloping-induced Vibrations

The general non-dimensional mass-damping parameter proposed in Equation 2.1 may also be used in galloping response predictions. Assuming that the driving force is proportional to the along-wind depth, d, gives the following onset wind velocity of galloping, v_{CG}, (Hansen, 2011)

$$v_{CG} = 2Sc_G n_e b/a_{GG},$$

where n_e is the natural frequency of structure and a_{GG} is the factor of galloping instability corresponding to the use of the general mass-damping parameter, Sc_G,

$$a_{GG} = -\left(\frac{\mathrm{d}C_L}{\mathrm{d}\theta} + C_D\right), \tag{2.2}$$

which is based on an aerodynamic damping estimate of

$$\delta_{aG} = -\frac{\rho d v_m}{4 m_e n_e} a_{GG}, \tag{2.3}$$

where C_D and C_L are the force coefficients for drag and lift respectively, using the in-wind depth as a reference length, and θ is the angle of incidence of the wind. The onset wind velocity of galloping corresponds to a total damping

of zero occurring when the negative aerodynamic damping becomes equal to the structural damping.

The Eurocode specifies a factor of galloping instability a_G from 0.4 to 2.0 for rectangular cross sections with the ratio of d/b in the range of 1/3 to 2, and these values are based on the traditional Scruton number definition. The similar galloping instability factor of a_{GG} based on the general non-dimensional mass-damping parameter will be in a much more narrow range of 1.0 to 1.5. Thus, the tendency described above for vortex-induced vibrations is also found for galloping-induced vibrations. For the 1 : 2 cross section with an in-wind depth being twice the cross-wind dimension, the Eurocode factor a_G of galloping instabilities referring to the Scruton number is 2.0 corresponding to a_{GG} values in Eq. 2.2 of 1.0.

2.6.4 Aeroelastic Effects for 1:2 Cross Section

The results presented below are from a wind tunnel study focusing on aeroelastic effects of the 1:2 cross section with an in-wind depth being twice of the cross-wind dimension. The cross section 1 : 2 with an along-wind depth twice the cross-wind dimension was tested in low turbulent flow with an intensity of approx. 2% – see the results presented in Figures 2.18 to 2.20. From Figures 2.18 the galloping instability factor, a_{GG} has been found to be 4.3 at zero angle of attack corresponding to wind perpendicular to the small side of the cross section.

For the 1:2 cross section both vortex shedding and galloping gives contributions to the aerodynamic damping. In the simplest form the two contributions of aerodynamic damping are assumed independent, and the total aerodynamic damping, δ_a, is expressed by

$$\delta_a = \delta_{KaG} + \delta_{aG}, \tag{2.4}$$

where δ_{KaG} and δ_{aG} are the aerodynamic damping originating from vortex shedding and galloping, respectively. Figure 2.19 shows the aerodynamic damping determined by subtracting the structural damping from the total damping measured, and the vortex-induced aerodynamic damping has been determined by Eq. 2.4 assuming that the aerodynamic damping from galloping follows Eq. 2.3. For an aerodynamic damping due to vortex shedding of 2 to 3% shown in Figure 2.19, the non-dimensional damping parameter (Hansen, 2013)

$$K_{aG} = \frac{\delta_{KaG}}{2\pi} \frac{m_e}{\rho\, bd}$$

becomes equal to between 1.8 and 2.7. It is promising to observe that this value of the aerodynamic damping parameter is in good agreement with the values of 2.4 and 2.7 found for cross sections of 2:1 and 1:1, respectively (Hansen, 2013).

In Figure 2.20 measurements of a rectangular cylinder with a cross section are shown together with estimated values for the onset galloping velocity from the Eurocode and ISO. The vibrations start around the resonant velocity for vortex shedding and continue to grow almost linearly with increasing wind velocity. The anticipated development of the response due to vortex shedding cannot be seen within the band of mass-damping parameters tested. This agrees with results obtained by Itoh and Tamura (2002), Kawai (1992) and Washizu et al. (1978). It may be seen that relative large differences in Sc_G do not yield significant differences in response and that the onset galloping velocity is independent of Sc_G and depends only on the Strouhal number.

For larger Sc_G , $Sc_G > 50$, separation between vortex-induced vibrations and galloping have been seen, and for really small Sc_G, $Sc_G < 3$, vortex-induced vibrations have been seen at v/nb equal to approximately 6 – see Itoh and Tamura (2002) and Washizu et al. (1978).

Figure 2.20 shows that the Eurocode prediction of the onset wind velocity for galloping is unsafe for general non-dimensional mass-damping parameters larger than approximately 9. For mass-damping parameters in the range of 9.5 to 39.5, the response starts to increase for reduced wind velocities of approximately 15. The most extreme deviation between the Eurocode and the test results occurs for a general mass-damping parameter of 39.5. The Eurocode onset wind velocity of galloping corresponds to a reduced wind velocity of $2 \times 39.5 = 79$, where the test results show initiation of galloping instabilities for a reduced wind velocity of approximately 15, i.e. at a wind velocity being approximately 5 times smaller than the Eurocode predictions.

With the higher a_{GG} of 4.3 based on Figure 2.18, the predictions fits well with the measured data except if the mass-damping-parameter is really small. The reason for this can be found in Figure 2.19. Here it can be seen that before the critical velocity there is a damping effect of the vortices. Thus the model will stay still until resonance speed is reached and start vibrating from there with increasing wind speed. Figure 2.19 also shows that galloping becomes the only driving force at $v/nb \gtrsim 20$, where the aerodynamic damping due to vortex shedding becomes zero. At the highest mass-damping parameter number the damping is so large that the vortex induced vibrations are suppressed, and therefore the model starts to vibrate at the onset galloping velocity. ISO 4354:2009 is seen to agree well with the measurements for all mass-damping parameters.

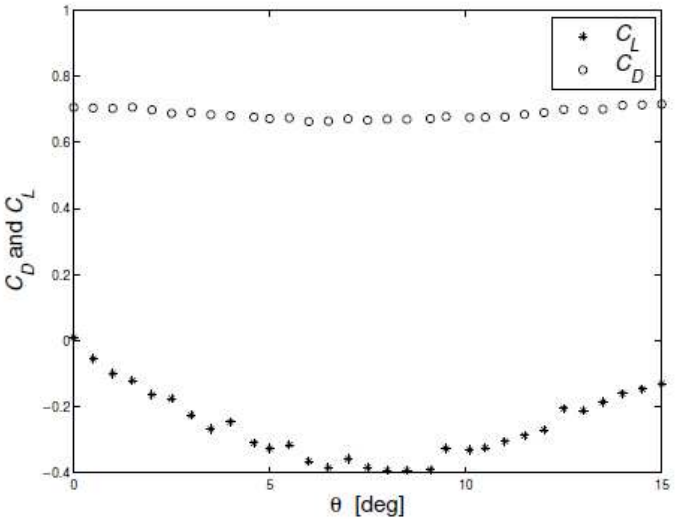

Figure 2.18: The lift and drag coefficient as a function of angle of attack. In-wind depth is used as a reference length for both the drag and lift coefficients.

The Eurocode specifies that interaction effects between vortex shedding and galloping are likely to occur when the calculated onset wind velocity of galloping is in the range of $0.7v_r$ to $1.5v_r$, where v_r is the resonance wind velocity for vortex shedding. The measuring results shown in Figure 2.20 indicate that this range should be much larger for the 1:2 cross section.

2.7 Design Criteria

For the dimensioning criteria reference is made to the code parts on different materials, such as steel, concrete and timber. In the present planned Eurocode revision, a focus area is wind loads relevant for structures, where their resistance increases for shorter load durations, e.g. glass panels.

The present codes represent the wind action on a structure by an equivalent static wind load calculated by the procedures outlined above. This static wind load is used to calculate structural stresses to be compared with the resistance specified in the code parts on different materials, such as steel, concrete, timber and glass. Most materials experience an increased resistance

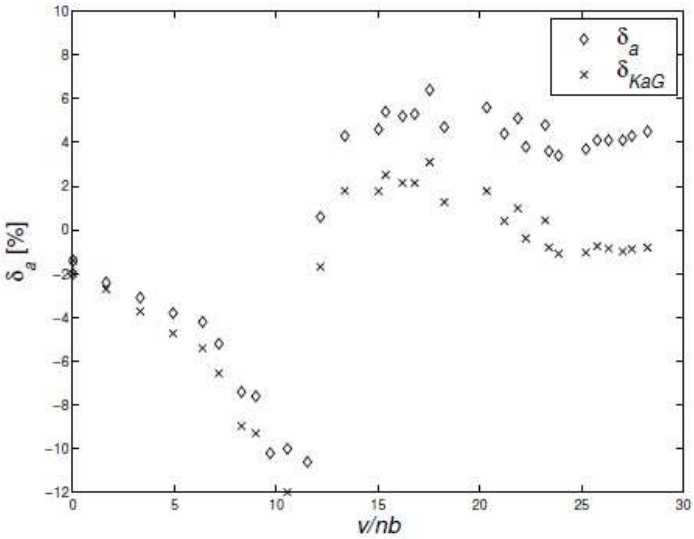

Figure 2.19: Negative aerodynamic damping – positive y-values – expressed by a logarithmic decrement. δ_{KaG} is the negative vortex-induced aerodynamic damping estimated by subtracting the galloping-induced aerodynamic damping from the total aerodynamic damping, δ_a, originating from both vortex shedding and galloping.

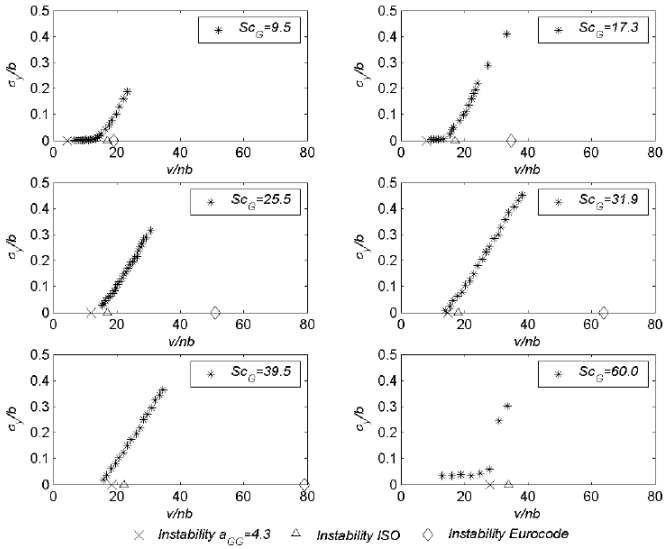

Figure 2.20: Wind-induced vibrations at different mass-damping parameters together with the predictions from the Eurocode EN 1991-1-4:2005 and ISO 4354:2009. The Eurocode and ISO instabilities described by the onset wind velocity of galloping are indicated by the markings on the x-axis.

when the load fluctuates fast. The time constants may be different indicating that the importance depends on the load in question. Future codes are expected to focus much more on the structural resistance relevant for fluctuating wind effects. Some examples relevant for ultimate limit states are described below.

Most steel structures are very ductile, and wind effects may initiate yielding, but the short duration of the extreme wind effects are not able make the structure collapse. Typically, for lattice structures the governing load situation is the wind-induced compression forces in the structural members. Besides permanent actions these compression forces originate from mean wind load and the influence of background turbulence and resonance turbulence. The mean wind load acts over 10 minutes and the effects of background turbulence often have frequencies of the order of 0.1 Hz corresponding to typical time periods of 10 seconds, and these durations seem to be relatively long compared to the response time of the lattice structure. However, the resonance

turbulence giving vibrations at the natural frequency, which for the lattice structure typically is of the order of 1 Hz, may have duration too short for an actual collapse to develop.

For glass panels experiments have been carried out with an experimental arrangement as shown in Figure 2.21. The glass plate, which is subject to the test, is placed on an iron frame. Underneath the plate is placed a strain gauge force transducer, on a piston pulling in the glass plate with a given force. The pressure is delivered by a 10 bar compressor, which is not shown in the picture. The static tests of two types of glass panels have been carried out by increasing the load gradually in cycles, and then unloading the glass plate. The dynamic tests of the glass have been carried out by repeating the load in series of 100 repetitions. This is done repeatedly until the glass panels fail.

The tests carried out showed that the failure when the fluctuating wind loads were applied were approximately twice the failure load for static conditions. Further testing will provide more statistical information on glass resistance, and it will enable the background for establishing appropriate load duration specifications in the European wind code.

If more accurate design criteria are established following the ideas described above, appropriate partial safety factors taking all relevant uncertainties of the wind load chain properly into account should be determined by detailed calibration studies, see chapter 2. These studies may give slightly increased partial safety factors expected to remove only a minor part of the increased structural resistance obtained by the more advanced design criteria described above.

2.8 Conclusion

The present wind loading design codes have reached a stage where they provide specifications that typically only deviate slightly. However, further harmonization is still needed, and a number of focus areas should be addressed in future revisions. Some of these focus areas are a consistent approach for determining the influence of both load duration and spatial averaging on pressure coefficients, wind loads on two skin façades and influence lines or mode shapes with changing sign.

Preferably, the codes should be transparent and this is not always the situation. A considerable improvement in the quality of building codes, including the Eurocode, is possible if a quality check is done before data are selected to be included. The quality check should consider the following items:

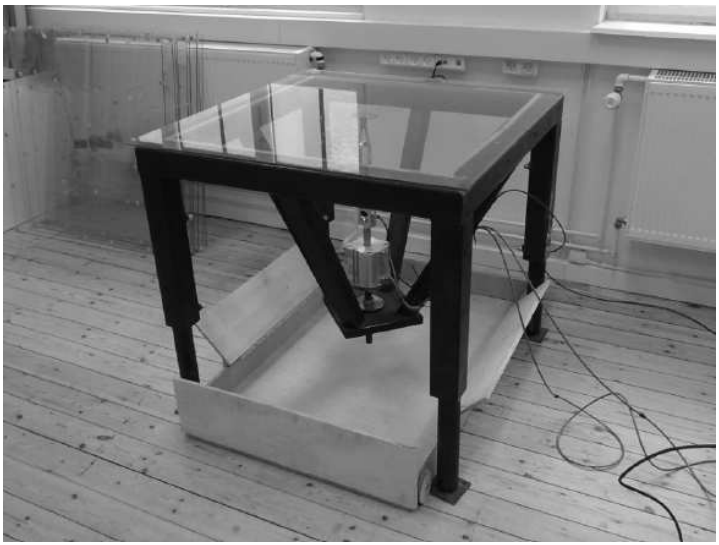

Figure 2.21: Experimental arrangement for testing glass resistance as function of load duration.

- Building codes should be probability based, so data used in the codes should also be probability based.
- The analysis techniques should be consistent with the choices made for the level of safety in the building codes.
- Values of the pressure coefficients in codes should be based on analysis of extreme values.
- The relation between averaging time and spatial averaging time and the choice of extreme value analysis should be consistent with the probabilistic approach applied.
- Flow conditions and measurements techniques should be known and within the range of applicability of the codes.

The general non-dimensional mass-damping parameter described in the paper will be a helpful design parameter used to predict whether structures may be sensitive to vortex-induced and galloping-induced vibrations. The use of the general non-dimensional mass-damping parameter instead of the Scruton number normally applied may reduce the uncertainties involved in code predictions of vortex-induced vibrations and galloping-induced vibrations considerably.

The combined effects of vortex shedding and galloping will for some cross sections give larger vibrations than predicted by the Eurocode. Improved theoretical models may be the basis for subsequent Eurocode updates taking this phenomenon more accurately into account.

Acknowledgements

The allowance of using the model scale results presented and the help of my colleagues at Svend Ole Hansen ApS and SOH Wind Engineering LLC preparing the wind tunnel tests carried out are greatly acknowledged.

References

R. Bashor and A. Kareem. Comparative study of major international standards. In *Proceedings of the Seventh Asia-Pacific Conference on Wind Engineering, November 8-12, Taipei, Taiwan.*, 2009.

N. J. Cook. *The designers guide to wind loading of building structures. Part 2: Static structures.* Building Research Establishment, 1985.

A. G. Davenport. The response of slender, line-like structures to a gusty wind. *Proceedings of the Institution of Civil Engineers*, 23:389–408, 1962.

A. G. Davenport. Gust loading factors. *Journal of the Structural Division, ASCE*, 93(3):11–34, 1967.

A. G. Davenport and N. Isuymov. The application of the boundary layer wind tunnel to the prediction of wind loading. In *Wind Effects on Buildings and Structures, Toronto*, pages 201–230, 1968.

C. Dyrbye and S. O. Hansen. *Wind loads on structures*. John Wiley & Sons, 1996.

ECCS. *Recommendations for calculating the effect of wind on constructions, 2nd Edition*. European Convention for Constructional Steelwork, 1987.

C. Geurts, B. Zimmerli, S. Hansen, P. Van Staalduinen, G. Sedlacek, M. Hortmanns, P. Spehl, and P. Blackmore. Transparency of pressure and force coefficients. *Proceedings of 3rd European and African Conference on Wind Engineering, Eindhoven, The Netherlands, July 2–6*, pages 165–172, 2001.

S. Hansen, P. Blackmore, C. Geurts, M. Hortmanns, G. Sedlacek, P. Spehl, P. Staalduinen, and B. Zimmerli. Eurocode procedures for predicting vortex excitation. In *Proceedings of 3rd European and African Conference on Wind Engineering, Eindhoven, The Netherlands, July 2–6*, 2001.

S. O. Hansen. Vortex-induced and galloping-induced vibrations of simple structures. In *Proceedings of the International Conference on Wind Engineering, Amsterdam, The Netherlands*, 2011.

S. O. Hansen. Vortex-induced vibrations the Scruton number revisited. *Structures and Buildings Journal – Institution of Civil Engineers*, 2013.

S. O. Hansen and S. Krenk. Dynamic along-wind response of simple structures. *J. Wind Eng. Ind. Aerod.*, 82(1):147–171, 1999.

E. Hjorth-Hansen and A. Kyrkjeeide. Aeroelastic response of a square tower model having solid or perforated walls. In *The University of Trondheim, Norway*, 1978.

J. Holmes, Y. Tamura, and P. Krishna. Comparison of wind loads calculated by fifteen different codes and standards, for low, medium and high-rise buildings. In *Proceedings of the 11th Americas Conference on Wind Engineering, San Juan, Puerto Rico, June 22-26*, 2009.

Y. Itoh and T. Tamura. The role of separated shear layers in unstable oscillations of a rectangular cylinder around a resonant velocity. *J. Wind Eng. Ind. Aerod.*, 90(4):377–394, 2002.

M. Jensen. *The model-law for phenomena in natural wind*. 1958.

H. Kawai. Vortex induced vibration of tall buildings. *J. Wind Eng. Ind. Aerod.*, 41 (1):117–128, 1992.

C. Scruton. On the wind-excited oscillations of stacks, towers and masts, 1963.

C. Scruton. *An introduction to wind effects on structures*. Oxford University Press, Engineering Design Guides 40, 1981.

G. Solari. Gust buffeting. I: Peak wind velocity and equivalent pressure. *Journal of Structural Engineering*, 119(2):365–382, 1993a.

G. Solari. Gust buffeting. II: Dynamic alongwind response. *Journal of structural*

engineering, 119(2):383–398, 1993b.

T. Stathopoulos. *Turbulent wind action on low-rise buildings*. PhD thesis, The University of Western Ontario, London, Ontario, Canada, 1979.

T. Vrouwenvelder and N. Scholten. Assessment criteria for existing structures. *Structural Engineering International*, 20(1):62–65, 2010.

K. Washizu, A. Ohya, Y. Otsuki, and K. Fujii. Aeroelastic instability of rectangular cylinders in a heaving mode. *J. Sound and Vibration*, 59(2):195–210, 1978.

B. Zimmerli. Process of drafting the Eurocode on wind action. In *Proceedings of the Third European & African Conference on Wind Engineering. Eindhoven, The Netherlands, July 2-6*, pages 157–163, 2001.